Gait & Posture 74 (2019) 27–32

Contents lists available at ScienceDirect

Gait & Posture

journal homepage: www.elsevier.com/locate/gaitpost

Full length article

The increase of joint contact forces in foot joints with simulated subtalar fusion in healthy subjects

Yongcheol Kim[a], Jeongwon Kim[b], Kyoung Min Lee[c], Seungbum Koo[d,*]

[a] Agency for Defense Development, Daejeon, Republic of Korea
[b] School of Mechanical Engineering, Chung-Ang University, Seoul, Republic of Korea
[c] Department of Orthopedic Surgery, Seoul National University Bundang Hospital, Seongnam, Republic of Korea
[d] Department of Mechanical Engineering, Korea Advanced Institute of Science and Technology, 291 Daehak-ro, Yuseong-gu, Daejeon, 34141, Republic of Korea

ARTICLE INFO

Keywords:
Joint contact force
Foot joint kinematics
Musculoskeletal simulation
Subtalar fusion
Gait

ABSTRACT

Background: Subtalar fusion usually leads to a satisfactory clinical outcome by eliminating the motion of the subtalar joint but can cause an aggravation of osteoarthritis after the subtalar fusion. Previous studies have investigated the effect of subtalar fusion in static testing using cadaver limbs, but there was no evidence of an aggravation of osteoarthritis.
Research question: The objective was to investigate the differences in foot joint kinematics and kinetics during a standing pose and walking with and without subtalar fusion, using a musculoskeletal simulation.
Methods: Full-body joint kinematics, ground reaction force, and foot pressure of the healthy subjects were recorded during walking using an optical motion capture system. The models with and without subtalar fusion were constructed using the AnyBody Modeling System (AnyBody Technology, Aalborg, Denmark). The range of motion and contact forces in the individual foot joints with and without simulated subtalar fusion in healthy subjects were estimated using computational simulation and compared using the Wilcoxon signed-rank test. The change of motion in the Chopart's joint was observed.
Results: Normalized to the subject's body weight (BW), the average maximum contact forces in the tibiotalar and Lisfranc joints during walking were significantly increased by 2.6 and 0.9 BW with the simulated subtalar joint fusion, respectively. The simulated subtalar joint fusion increased joint contact forces significantly during walking, which can increase the risks of secondary arthritis in the adjacent joints.
Significance: The subtalar joint fusion increased the joint contact forces in adjacent joints during walking implying that the fusion can increase the risk of secondary injuries in adjacent joints in the foot.

1. Introduction

The subtalar joint between the talus bone and the calcaneus bone plays a significant role in transmitting the body's load to the foot and helps provide efficient and stable ankle kinematics during walking [1]. Surgery is considered in the case of an abnormality in the subtalar joint that did not respond to conservative treatment [2]. Subtalar fusion by inserting a screw between the talus and the calcaneus is often preferred to alleviate the symptoms of the patients suffering from severe pain or deformity of the foot joint in weight bearing. Isolated subtalar joint fusion is a widely accepted treatment for diagnoses such as post-traumatic arthrosis, osteoarthritis, talocalcaneal coalition, and inflammatory foot joint disease [3], and fair clinical outcomes in patients were reported with respect to subtalar fusion in evaluation studies [4,5].

However, although subtalar joint fusion usually leads to a satisfactory clinical outcome, the fusion can cause secondary osteoarthritis in other joints [68]. A risk of secondary osteoarthritis in adjacent joints after subtalar joint fusion was reported in long-term follow-up studies [8]. The rate of secondary osteoarthritis in the tibiotalar joint after subtalar joint fusion was up to 30% in a review of the published literature [8]. Furthermore, even in forefoot joints, postoperative sequelae requiring additional surgical treatment has occurred after subtalar fusion [6].

The effect of a subtalar fusion on the biomechanics of adjacent foot joints was investigated using cadaveric feet [2,9]. The hindfoot triple fusion increased contact stresses in the tibiotalar joint in cadaveric specimens [9]. Isolated subtalar fusion in cadaveric feet decreased contact force and areas under static conditions [2]. Meanwhile, knowledge of the change of kinematics and kinetics in the foot during

* Corresponding author.
E-mail address: skoo@kaist.ac.kr (S. Koo).

https://doi.org/10.1016/j.gaitpost.2019.07.376
Received 30 January 2019; Received in revised form 24 July 2019; Accepted 26 July 2019

motion, such as while walking after subtalar fusion, is necessary to help understand the mechanisms of secondary injuries. Changes of joint kinematics and foot pressure with subtalar fusion during walking were analyzed in previous studies [10,11]. Tibiotalar and subtalar joint fusions changed the net ankle moment during walking [11].

The joint contact forces acting on the foot and ankle joints are key factors to consider in the progression of osteoarthritis [12]. Internal biomechanics during daily activities can be predicted from measured kinematics and external forces using computational simulation methods. The effect of spinal fusion in adjacent spinal joints was studied using musculoskeletal simulation [13]. In addition, recently, a detailed foot model has been introduced that can predict joint reaction forces at the tibiotalar [12,14], calcaneocuboid [15], tarsometatarsal, and metatarsophalangeal (MTP) joints [16] during walking.

The aim of this study was to estimate the contact forces in foot joints during walking, using a musculoskeletal dynamic simulation of a multi-segment foot model to understand the effect of subtalar fusion on foot kinetics. It was hypothesized that subtalar joint fusion would lead to increased joint contact forces in the tibiotalar joint and adjacent foot joints due to changed foot kinematics after subtalar joint fusion during walking when compared with that in intact feet. Subtalar fusion was simulated in healthy subjects.

2. Methods

2.1. Data acquisition

This study was approved by the Chung-Ang University Institutional Review Board, and written consent was obtained from each subject before testing. Kinematics, ground reaction forces (GRF), and foot pressure data were collected from 10 healthy subjects (all males, age 24.7 ± 1.2 years, height 176.5 ± 4.4 cm, and body weight 72.9 ± 7.9 kg). They walked barefoot at a self-selected walking speed on a walkway with a force plate (AMTI OR-6, Advanced Mechanical Technology, Inc., Watertown, MA USA). A pressure mat (FDM-S, zebris Medical GmbH, Isny im Allgäu, Germany) was placed on top of the force plate with a thin rubber sheet between them to minimize slip between them. The plug-in gait marker set and the Oxford Foot Model marker set were placed on each subject, and marker trajectories were recorded using an electronic optical motion capture system with six cameras at 100 Hz (MX T-10, Vicon Motion Systems Ltd., Oxford, UK). Simultaneously, GRF and foot pressure were recorded at 1000 and 500 Hz, respectively. The kinematics, GRF, and foot pressure data were synchronized and resampled at 100 Hz, which were then further processed from heel-strike to toe-off during the stance phase of walking. Additionally, standing-pose data were collected with the same experimental protocol.

2.2. Musculoskeletal model

We recently developed a five-segment musculoskeletal foot model by modifying the detailed foot model in the AnyBody Managed Modeling Repository [16] and integrated it with a full-body musculoskeletal model for quantifying moments in foot joints [17]. This five-segment foot model consists of five rigid segments (talus, calcaneus, midfoot, metatarsals, and toes) and five joints (tibiotalar, subtalar, Chopart's, Lisfranc, and MTP joints), as shown in Fig. 1. The foot model has nine rotational degrees of freedom, including flexion/extension at the tibiotalar, Chopart's, Lisfranc, and MTP joints; abduction/adduction at the Chopart's, Lisfranc, and MTP joints; and inversion/eversion at the subtalar and Chopart's joint. Twenty-one muscles and 17 ligaments were incorporated in the skeletal model. The predicted temporal patterns of the muscle excitation level were compared with that in previous electromyographic studies. The tibialis anterior muscle was activated at around 10% of the stance phase similar to that in a previous study [16], and the excitation level of the tibialis posterior muscle was the highest immediately after heel strike during the stance phase of walking similar to that in a previous study [18]. The predicted joint contact forces also agreed with that shown in previous studies [14,16]. The inversion/eversion degree of freedom at the subtalar joint was removed to represent a subtalar-fused foot model.

2.3. Musculoskeletal simulation

The measured body marker trajectories were input into the full-body template model with our five-segment foot model. The kinematics of the joints were estimated in the kinematics optimization routine in the AnyBody Modeling System by matching the marker locations on the model to those on a subject [19]. The trajectories of 20 markers on the leg, including 12 markers on the foot, determined the kinematics of the lower limb and foot joints. We referred to a previous study [20] for anatomical landmarks for marker positions. Scales of the five foot-segments and marker positions were adjusted to minimize the difference between the marker locations on the model and the trajectories of the markers on each subject in the kinematics optimization routine. The markers attached to each segment and the adjustable directions of each marker are shown in Fig. 2A. Markers with a low observer (or placement) error such as D5MT (the distal end of the fifth metatarsal) were excluded from optimization. Additionally, nine markers were placed on each leg as shown in Table 1. Each bone segment in the foot model was linearly and uniformly scaled in all three orthogonal directions. The attachment points of the muscles and ligaments were adjusted according to the scaled shapes of the bone segments. The initial lengths of the muscles and ligaments were adjusted according to the scaling of the foot geometry while maintaining the muscle strength and ligament stiffness.

The GRF measured at the center of the foot pressure was divided by the ratio of the sum of the pressure under each foot segment [21]. To input distributed GRFs into the foot segments, multiple nodes were attached to each foot segment (calcaneus: 31, midfoot: 36, metatarsals: 73, and toes: 30), and the total number of nodes was 170 as illustrated in Fig. 2B. The nodes in a segment could provide the GRF that was distributed to the segment using foot pressure data. To synchronize the coordinate systems between the pressure mat and the force input nodes in the model, the position of each cell on the pressure mat was transformed to the motion capture coordinate system using markers attached to the four corners of the pressure mat. The distributed forces of the cells in the pressure mat were transmitted to the closest foot node estimated from the kinematics optimization routine.

Joint kinematics and distributed GRFs were input to the full-body musculoskeletal model with our custom foot. An inverse dynamics-based optimization in the AnyBody Modeling System was performed at each instance of the input data to estimate the kinetics of the human musculoskeletal system, which included forces of the muscles and ligaments. The optimization routine minimized the maximum activation levels (force divided by strength) of the muscle actuators [22]. The force between two adjacent bones was calculated at each joint in Fig. 1 during the kinetics estimation routine.

2.4. Statistical analysis

Temporal forces of muscles around the ankle and joint contact forces in the tibiotalar, Chopart's, Lisfranc, and MTP joints of intact and subtalar-fused feet were estimated during a standing pose and in the stance phase of walking of 10 subjects. All force data were normalized by the subject's body weight (BW). The data did not have normal distribution according to the Shapiro-Wilk test. Thus, the two groups were compared using the Wilcoxon signed-rank test. The normalized muscle forces and normalized joint contact forces of the two groups were compared at 11 equally spaced discrete timepoints (or every 10%) of the stance phase [23] with the Wilcoxon signed-rank test (matched pairs) with statistical significance established using a P-value of 0.05/

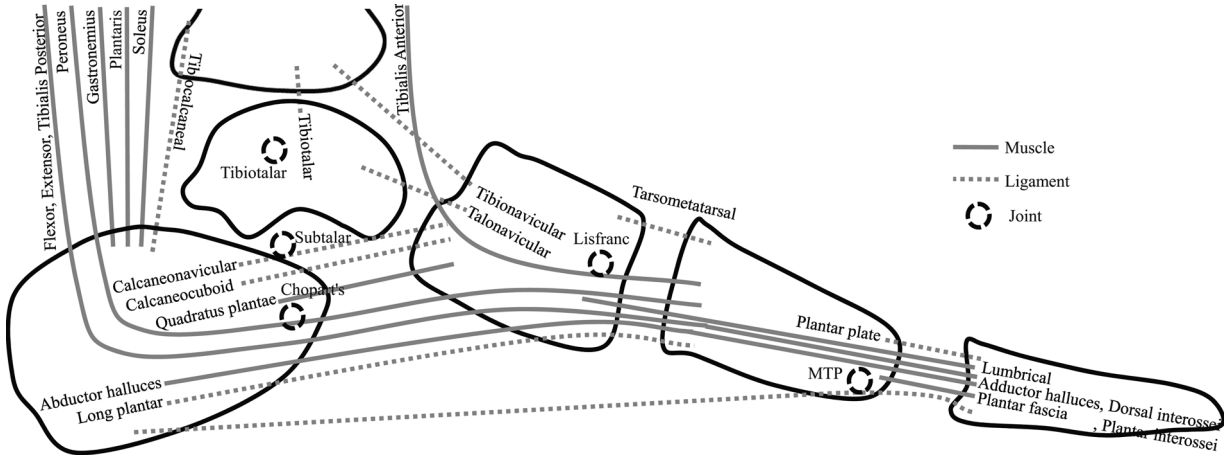

Fig. 1. The structure of the foot model consists of five segments, five joints, 21 muscles, and 17 ligaments.

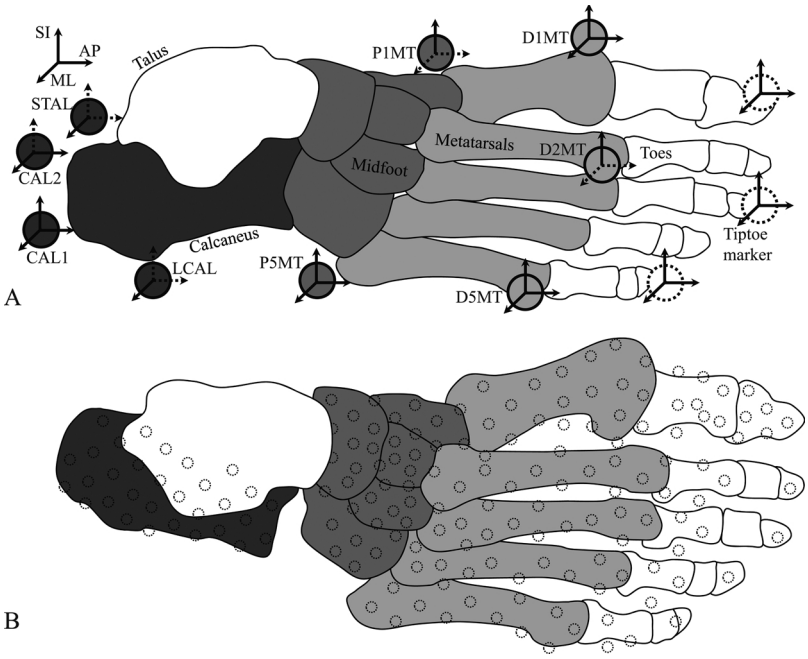

Fig. 2. (A) Nine skin markers from the Oxford Foot Model and three additional markers at the tips of the toes were attached on the five-segment foot model. The color of the markers represents a rigid body group of segments. The arrows with dashed lines show the directions to be adjusted during the kinematics optimization routine, (B) The nodes in a segment could provide the ground reaction force (GRF) that was distributed to the segment.

Table 1
Average (one standard deviation) range of motion (ROM) in degrees for the foot joints around the talus during stance of walking in intact and subtalar-fused foot models (Flex.: Flexion, Ext.: Extension, Inv.: Inversion, Eve.: Eversion, Abd.: Abduction, Add.: Adduction).

Joint	Ankle	Subtalar	Chopart's		
ROM	Flex./Ext.	Inv./Eve.	Flex./Ext.	Abd./Add.	Inv./Eve.
Intact foot model	15.6 ± 3.7	8.1 ± 2.0*	23.8 ± 4.1*	7.2 ± 1.6	8.5 ± 3.7
Subtalar-fused model	16.1 ± 2.3	0.0 ± 0.0*	26.7 ± 4.2*	8.4 ± 3.7	5.7 ± 1.8

* Significantly different between the intact and subtalar-fused model (P-value < 0.05).

11 = 0.0045 with Bonferroni correction. Maximum joint contact forces in each foot joint during the stance phase of the two groups were also compared. To test the differences in the joint kinematics, the range of motion (ROM) of the tibiotalar, subtalar, and Chopart's joints along the three orthogonal axes were estimated and compared between the two groups using the Wilcoxon signed-rank test. Statistical analyses were performed using IBM SPSS Statistics for Windows (version 23; IBM Corp., Armonk, NY, USA) with statistical significance established at a P-value < 0.05 for all comparisons.

3. Results

The ROM of subtalar inversion/eversion was 8.1 ± 2.0 degrees in the intact foot model, which was significantly higher than that in the subtalar-fused foot model. Among the joints around the talus, the subtalar fusion significantly increased only the Chopart's flexion/extension ROM by 2.9 degrees, as shown in Table 2.

The forces of the muscles around the ankle during the stance phase of walking were estimated in the dynamic simulation and are presented in Fig. 3. The forces in the peroneus muscle, an ankle plantar flexor, and the extensor digitorum longus muscle, an ankle dorsiflexor, were significantly increased at the late stance phase in the subtalar-fused model. The maximum force of the peroneus muscle ranged from 0.2 to 5.1 BW in the intact model and from 0.7 to 6.3 BW in the subtalar-fused model during the stance phase. The maximum force of the extensor digitorum longus muscle ranged from 0.3 to 2.3 BW in the intact model and from

Table 2
Average (one standard deviation) joint contact forces normalized by body weight in the ankle, Chopart's, Lisfranc, and MTP joints during the standing pose.

Joints	Intact foot model	Subtalar-fused model
Ankle	2.4 ± 0.9*	2.3 ± 0.8*
Chopart's	0.8 ± 0.5	0.8 ± 0.4
Lisfranc	1.0 ± 0.5	1.0 ± 0.5
MTP	1.1 ± 0.4	1.1 ± 0.4

* Significantly different between the intact and subtalar-fused model (P-value < 0.05).

0.4 to 5.4 BW in the subtalar-fused model.

The joint contact force in the tibiotalar joint had a significant increase of 1.7 BW on average during 80–90% of the stance phase of walking, as shown in Fig. 4. The maximum tibiotalar joint contact force increased from 8.7 ± 3.0 BW to 11.3 ± 3.1 BW. The joint contact forces in the Lisfranc joint with subtalar fusion had significant increases during the 80–100% of the stance phase by an average 0.5 BW. The maximum Lisfranc joint contact force increased from 2.6 ± 1.2 BW to 3.5 ± 1.7 BW.

The joint contact forces during a standing pose were also obtained. The average joint contact forces in the tibiotalar joint in the intact foot model and subtalar-fused model were 2.4 and 2.3 BW, respectively. The joint contact forces in the tibiotalar joint were significantly decreased with subtalar fusion by 0.1 BW, while the joint contact forces in the Chopart's, Lisfranc, and MTP with both models were 0.8, 1.8, and 1.1 BW, respectively.

4. Discussion

A musculoskeletal model of the foot and ankle was constructed to understand the kinematic and kinetic changes during walking in the foot and ankle after subtalar fusion, using a simulation method. Significant changes in foot kinematics, muscle forces, and joint contact forces were observed between the model with subtalar fusion and without subtalar fusion.

Subtalar fusion caused changes in the motion of the Chopart's joint adjacent to the subtalar joint. An increase of the ROM in the adjacent foot joint after subtalar fusion during static pose was reported in a cadaveric study [2], while there are no reported studies on patients with subtalar fusion using a multi-segment foot model. Wu et al. (2005) [10] reported changed kinematics in major joints such as the hip and knee after subtalar fusion during walking. In the case of tibiotalar fusion, increased ROM in the forefoot joint during walking was observed in a previous study [24]. This was explained by the mechanism of kinematic compensation of a fused joint by the other joints. In our simulation results, the increased ROM of the Chopart's joint compensated for the foot mobility after subtalar fusion and changed the kinetics of the foot.

The contact force in the tibiotalar joint during walking was significantly increased in the subtalar-fused model. The difference in tibiotalar joint contact forces between the intact and subtalar-fused foot may have originated from an abnormal joint motion in the patients with a subtalar fusion. The motion of the subtalar joint plays a significant role in the pronation mechanism of the foot [25]. Pronation of the foot is the mechanism to attenuate the loading at the instant of ground contact during walking. The pronated foot helps the body's forward progression and adapts to irregular surfaces [26,27]. Decreased pronation of the foot in the subtalar-fused model impaired the stability of the body during walking. The plantar flexors, such as the soleus and peroneus which play important roles in body support and forward progression during walking [28], were overloaded to compensate for the lost stability. Increased tibiotalar joint contact force due to abnormal muscle contraction leads to secondary osteoarthritis after subtalar joint fusion. Our findings suggest that biomechanical changes during a dynamic condition in the subtalar-fused model could be related to secondary osteoarthritis in the tibiotalar joint after subtalar fusion.

Increased joint contact forces in the Lisfranc joints were also observed in the subtalar-fused model. Overloaded plantar flexor muscles resulted in increased joint contact forces in the distal foot joints. Co-activation of the antagonist was necessary to maintain joint stability [29]. The force of the ankle dorsiflexor, such as an extensor digitorum longus muscle, was increased, as the force of plantar flexors increased in the subtalar-fused model. An increase in the force of the dorsiflexor, which is connected to the toes, caused an increase in the distal joint contact force. In clinical studies, some patients with subtalar joint fusion had additional degenerative changes and underwent postoperative treatment in the calcaneocuboid and talonavicular joints in prospective

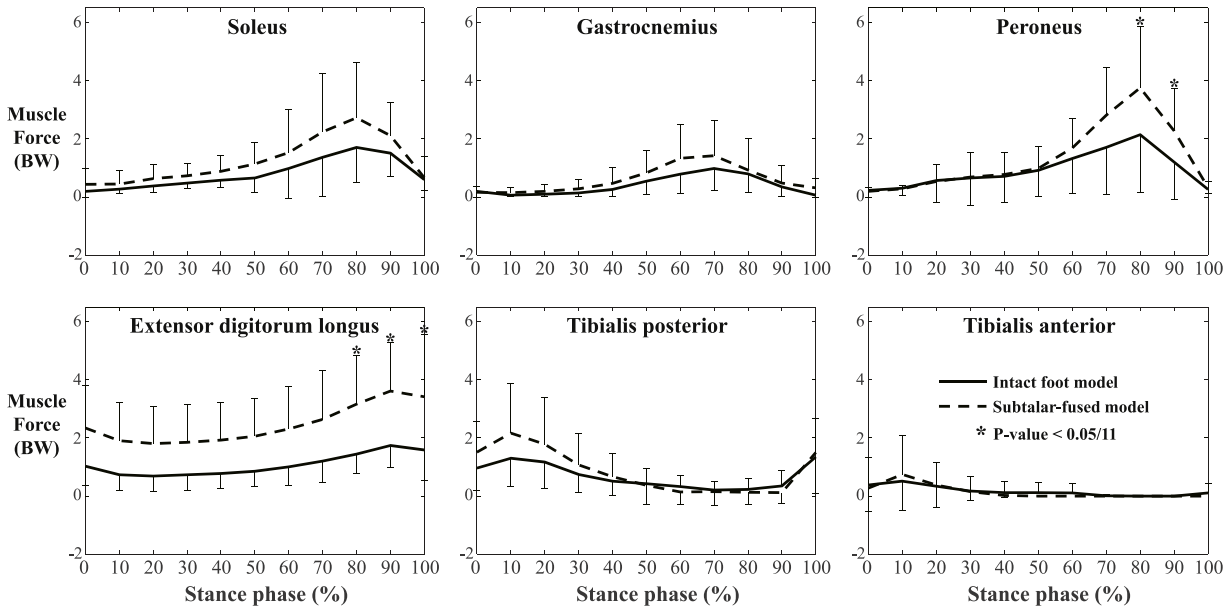

Fig. 3. Average (one standard deviation) soleus, gastrocnemius, peroneus, extensor digitorum longus, tibialis posterior, and tibialis anterior muscle forces normalized by the body weight of each subject during the stance phase of walking with 10% intervals (* P-value < 0.05/11).

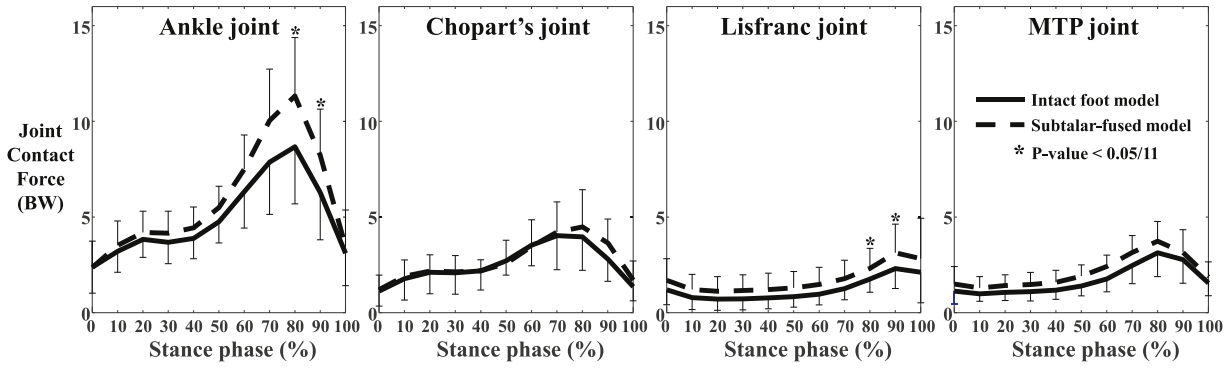

Fig. 4. Average (one standard deviation) joint contact forces normalized by the body weight of each subject in the tibiotalar, Chopart's, Lisfranc, and MTP joints during the stance phase of walking with 10% intervals (* P-value < 0.05/11).

studies [6,7]. This clinical outcome suggests that biomechanical changes in the distal joints occurs during daily activity after subtalar joint fusion. Thus, the clinician should carefully observe the distal joint during follow-up and prescribe orthotics to prevent increased contact force in the distal joint. It is necessary to understand the precise surgical technique to predict accurately the postoperative condition.

On the other hand, in our results, the joint contact forces in the Chopart's, Lisfranc, and MTP joints during the standing pose were not changed after subtalar joint fusion. The fusion of the subtalar joint removed the motion in the subtalar joint and set it at the original position. The tibiotalar joint contact force during the standing pose was significantly increased after fusion of the subtalar joint, but the amount of increase, while statistically significant, was very small. Hutchinson et al. (2016) [2] investigated the change of contact forces in the tibiotalar joint following subtalar fusion in a cadaveric study, but the tibiotalar joint contact pressure after subtalar joint fusion during the standing pose was decreased. In other words, an increase of contact stress after subtalar fusion was not shown in that study [2]. Subtalar fusion was verified as an effective treatment for hindfoot deformity correction in X-ray images during a standing pose [4]. In our results, the absolute change of the forces in the tibiotalar joint were small after fusion of the subtalar joint during the standing pose and may not affect degeneration in the tibiotalar joint as reported in a previous study [2].

A limitation of this study was that skeletal kinematics were obtained using only an optical motion capture system. Measuring talus bone movement using attached skin markers is difficult because it is not exteriorly palpable. Accurate subtalar joint kinematics were measured using a bi-planar fluoroscopy system in our previous study [1]. It was reported that subtalar joints gradually everted during the early stance phase, while they were inverted in the late stance phase, and the ROM of inversion/eversion in the subtalar joint was 6.6 ± 4.5 degrees. Our measurement of temporal patterns in the subtalar inversion/eversion motion agreed with those in our previous study [1], and ROM in the subtalar joint was similar to our previous findings. Another limitation is that the kinematics and kinetics in subtalar fusion were predicted with simulated subtalar fusion in healthy subjects. It is assumed that marker trajectories and GRFs will not change after subtalar fusion in patients. Although there is variation depending on the surgical technique used for fixing motion between the talus and the calcaneus bone [30], we assumed that joint motion was absolutely constrained after joint fusion.

In conclusion, we used musculoskeletal simulation to determine the muscle forces and joint contact forces in the foot joints with and without subtalar joint fusion during standing pose and walking. We found that subtalar joint fusion had little effect on joint forces during the static pose but it significantly increased the joint forces in adjacent joints during walking in our simulations, which could be the cause of an increase of secondary injuries such as osteoarthritis in adjacent joints after subtalar 6–8.

Declaration of Competing Interest

As far as the authors are aware, there are no conflicts of interest associated with this manuscript. This paper has been neither published nor submitted elsewhere for publication, in whole or in part, either in a serial or professional journal or as part of a book that is formally published and made available to the public.

Acknowledgments

This work was supported by the Projects for Research and Development of Police Science and Technology through the Center for Research and Development of Police Science and Technology and the Korean National Police Agency (PA-C000001), funded by the Ministry of Science and ICT of the Republic of Korea. This research was also supported by the Chung-Ang University Graduate Research Scholarship in 2018.

References

[1] S. Koo, K.M. Lee, Y.J. Cha, Plantar-flexion of the ankle joint complex in terminal stance is initiated by subtalar plantar-flexion: a bi-planar fluoroscopy study, Gait Posture 42 (2015) 424–429, https://doi.org/10.1016/j.gaitpost.2015.07.009.
[2] I.D. Hutchinson, J.R. Baxter, S. Gilbert, M.V. Hogan, J. Ling, S.M. Saunders, et al., How do hindfoot fusions affect ankle biomechanics: a cadaver model, Clin. Orthop. Relat. Res. 474 (2016) 1008–1016, https://doi.org/10.1007/s11999-015-4671-5.
[3] M.J. Best, L.T. Buller, A. Miranda, National trends in foot and ankle arthrodesis: 17-year analysis of the national survey of ambulatory surgery and national hospital discharge survey, J. Foot Ankle Surg. 54 (2015) 1037–1041, https://doi.org/10.1053/j.jfas.2015.04.023.
[4] H.B. Kitaoka, G.L. Patzer, Subtalar arthrodesis for posterior tibial tendon dysfunction and pes planus, Clin. Orthop. Relat. Res. (1997) 187–194.
[5] M.B. Davies, P.F. Rosenfeld, P. Stavrou, T.S. Saxby, A comprehensive review of subtalar arthrodesis, Foot Ankle Int. 28 (2007) 295–297, https://doi.org/10.3113/FAI.2007.0295.
[6] M.C. Glanzmann, R. Sanhueza-Hernandez, Arthroscopic subtalar arthrodesis for symptomatic osteoarthritis of the hindfoot: a prospective study of 41 cases, Foot Ankle Int. 28 (2007) 2–7, https://doi.org/10.3113/FAI.2007.0001.
[7] P. Joveniaux, A. Harisboure, X. Ohl, E. Dehoux, Long-term results of in situ subtalar arthrodesis, Int. Orthop. 34 (2010) 1199–1205, https://doi.org/10.1007/s00264-010-1041-5.
[8] M. Ebalard, G. Le Henaff, G. Sigonney, R. Lopes, G. Kerhousse, J. Brilhault, et al., Risk of osteoarthritis secondary to partial or total arthrodesis of the subtalar and midtarsal joints after a minimum follow-up of 10 years, Orthop Traumatol-Sur. 100 (2014), https://doi.org/10.1016/j.otsr.2014.03.003 S231-S7.
[9] A. Suckel, O. Muller, T. Herberts, P. Langenstein, P. Reize, N. Wulker, Talonavicular arthrodesis or triple arthrodesis - Peak pressure in the adjacent joints measured in 8 cadavar specimens, Acta Orthop. 78 (2007) 592–597, https://doi.org/10.1080/17453670710014275.
[10] W.L. Wu, P.J. Huang, C.J. Lin, W.Y. Chen, K.F. Huang, Y.M. Cheng, Lower extremity kinematics and kinetics during level walking and stair climbing in subjects with triple arthrodesis or subtalar fusion, Gait Posture 21 (2005) 263–270, https://doi.org/10.1016/j.gaitpost.2004.02.001.
[11] R.J. Weiss, E. Brostrom, A. Stark, M.C. Wick, P. Wretenberg, Ankle/hindfoot arthrodesis in rheumatoid arthritis improves kinematics and kinetics of the knee and hip: a prospective gait analysis study, Rheumatology. 46 (2007) 1024–1028, https://doi.org/10.1093/rheumatology/kem017.
[12] R.N. Stauffer, E.Y. Chao, R.C. Brewster, Force and motion analysis of the normal,

diseased, and prosthetic ankle joint, Clin. Orthop. Relat. Res. (1977) 189–196.
[13] D. Ignasiak, T. Peteler, T.F. Fekete, D. Haschtmann, S.J. Ferguson, The influence of spinal fusion length on proximal junction biomechanics: a parametric computational study, Eur. Spine J. 27 (2018) 2262–2271, https://doi.org/10.1007/s00586-018-5700-3.
[14] J.A.I. Prinold, C. Mazza, R. Marco, I. Hannah, C. Malattia, S. Magni-Manzoni, et al., A patient-specific foot model for the estimate of ankle joint forces in patients with juvenile idiopathic arthritis, Ann. Biomed. Eng. 44 (2016) 247–257, https://doi.org/10.1007/s10439-015-1451-z.
[15] V.L. Giddings, G.S. Beaupre, R.T. Whalen, D.R. Carter, Calcaneal loading during walking and running, Med. Sci. Sports Exerc. 32 (2000) 627–634, https://doi.org/10.1097/00005768-200003000-00012.
[16] A.A. Al-Munajjed, J.E. Bischoff, M.A. Dharia, S. Telfer, J. Woodburn, S. Carbes, Metatarsal Loading During Gait-A Musculoskeletal Analysis, J Biomech Eng-T Asme. (2016) 138, https://doi.org/10.1115/1.4032413.
[17] Y. Kim, K.M. Lee, S. Koo, Joint moments and contact forces in the foot during walking, J. Biomech. (2018), https://doi.org/10.1016/j.jbiomech.2018.04.022.
[18] G.S. Murley, K.B. Landorf, H.B. Menz, A.R. Bird, Effect of foot posture, foot orthoses and footwear on lower limb muscle activity during walking and running: a systematic review, Gait Posture 29 (2009) 172–187, https://doi.org/10.1016/j.gaitpost.2008.08.015.
[19] M.S. Andersen, M. Damsgaard, J. Rasmussen, Kinematic analysis of over-determinate biomechanical systems, Comput Method Biomec. 12 (2009) 371–384, https://doi.org/10.1080/10255840802459412.
[20] M.C. Carson, M.E. Harrington, N. Thompson, J.J. O'connor, T.N. Theologis, Kinematic analysis of a multi-segment foot model for research and clinical applications: a repeatability analysis, J. Biomech. 34 (2001) 1299–1307, https://doi.org/10.1016/S0021-9290(01)00101-4.
[21] B.A. MacWilliams, M. Cowley, D.E. Nicholson, Foot kinematics and kinetics during adolescent gait, Gait Posture 17 (2003) 214–224, https://doi.org/10.1016/S0966-6362(02)00103-0.
[22] J. Rasmussen, M. Damsgaard, M. Voigt, Muscle recruitment by the min/max criterion – a comparative numerical study, J. Biomech. 34 (2001) 409–415, https://doi.org/10.1016/S0021-9290(00)00191-3.
[23] C.H. Chen, J.S. Li, A. Hosseini, H.R. Gadikota, T.J. Gill, G. Li, Anteroposterior stability of the knee during the stance phase of gait after anterior cruciate ligament deficiency, Gait Posture 35 (2012) 467–471, https://doi.org/10.1016/j.gaitpost.2011.11.009.
[24] D.R. Sturnick, C.A. Demetracopoulos, S.J. Ellis, R.M. Queen, J.C.B. Kolstov, J.T. Deland, et al., Adjacent joint kinematics after ankle arthrodesis during cadaveric gait simulation, Foot Ankle Int. 38 (2017) 1249–1259, https://doi.org/10.1177/1071100717726806.
[25] T.G. McPoil, H.G. Knecht, Biomechanics of the foot in walking: a function approach, J. Orthop. Sports Phys. Ther. 7 (1985) 69–72.
[26] R.A. Mann, Surgical implications of biomechanics of the foot and ankle, Clin. Orthop. Relat. Res. (1980) 111–118.
[27] T.E. Clarke, E.C. Frederick, L.B. Cooper, Effects of shoe cushioning upon ground reaction forces in running, Int. J. Sports Med. 4 (1983) 247–251, https://doi.org/10.1055/s-2008-1026043.
[28] R.L. Wang, E.M. Gutierrez-Farewik, The effect of subtalar inversion/eversion on the dynamic function of the tibialis anterior, soleus, and gastrocnemius during the stance phase of gait, Gait Posture 34 (2011) 29–35, https://doi.org/10.1016/j.gaitpost.2011.03.003.
[29] R. Baratta, M. Solomonow, B.H. Zhou, D. Letson, R. Chuinard, R. Dambrosia, Muscular coactivation - the role of the antagonist musculature in maintaining knee stability, Am J Sport Med. 16 (1988) 113–122, https://doi.org/10.1177/036354658801600205.
[30] B. Hintermann, V. Valderrabano, B. Nigg, Influence of screw type on obtained contact area and contact force in a cadaveric subtalar arthrodesis model, Foot Ankle Int. 23 (2002) 986–991, https://doi.org/10.1177/107110070202301102.